

Modeling and performance analysis of Schottky barrier carbon nanotube field effect transistor SB-CNTFET

Abdelali Diabi¹ · Abdesselam Hocini¹ · Souheil Mouetsi^{1,2} · Djamel Khedrouche¹

Published online: 16 May 2017
© Springer Science+Business Media New York 2017

Abstract The performance of a Schottky barrier carbon nanotube field effect transistor (SB-CNTFET) has been analyzed by means of a compact model. We present a study of the physical and geometrical parameters and their effects on the static and dynamic performance of the SB-CNTFET. For the static regime, we determine the variations in the current–voltage characteristics for three values of the potential barrier and the influence of the barrier on the on-state current. Also, we report the effect of the oxide thickness on the static performance. The relationship between the current–voltage characteristics and the nanotube diameter for different values of drain–source voltage is investigated. For dynamic systems, we study the effect of the gate–source voltage, the chirality and the CNT diameter on the transition frequency. It has been observed that the performance of the SB-CNTFET can be significantly controlled by changing some physical and geometrical parameters of the device.

Keywords Carbon nanotube · SB-CNTFET · Compact modeling · Transistor

1 Introduction

Since the discovery of carbon nanotubes in 1991 by Iijima, fundamental and science technology have devoted much

attention to the investigation of the electronic transport through single-wall carbon nanotubes (SWCNTs) [1]. Experiments and theory have predicted that this material can be either metallic or semiconducting (SC). The extraordinary electrical properties of such individual CNTs can rival or even exceed the best performance of usual metallic or semiconducting materials [2–5]. Semiconductor nanotubes can be used as active elements in field-effect transistors (CNTFETs) and CMOS-like logic circuits using *n*- or *p*-type MOS-like FETs with Schottky or ohmic contacts [6, 7].

There are two main types of CNTFETs that are being currently studied, differing by their current injection methods. CNTFETs can be fabricated with ohmic or Schottky contacts. The type of the contact determines the dominant mechanism of current transport and device output characteristics. CNTFETs are mainly divided into Schottky barrier CNTFETs (SB-CNTFETs) with metallic electrodes, which form Schottky contacts [8–11] and MOSFET-like CNTFETs with doped CNT electrodes, which form ohmic contacts [11, 12]. In SB-CNTFETs, tunneling of electrons and holes from the potential barriers at the source and drain junctions constitutes the current. The barrier width is modulated by the application of gate voltage, and thus the transconductance of the device is dependent on the gate voltage [12–14].

MOSFET-like CNTFETs take advantage of the *n*-doped CNT as the contact. Potassium doped source and drain regions have been demonstrated, and the behavior of MOSFETs-like CNTFETs have been experimentally verified [12]. In this type of transistors, since the depletion length, in case of carbon nanotube, is a function of diameter of carbon nanotube and thickness of gate insulators, a potential barrier is formed at the middle of the channel for small values of these parameters [4]. Consequently, for these devices it is mainly the potential barrier between the contacts that controls the current [4].

✉ Abdesselam Hocini
hocini74@yahoo.fr

¹ Laboratoire d'Analyse des Signaux et Systèmes, Université Mohamed Boudiaf-M'sila, BP 166, route Ichebilia, 28000 M'Sila, Algeria

² Département de génie électrique, Faculté des Sciences et des Sciences Appliquées, Université Larbi Ben M'hidi-Oum El Bouaghi, Oum El Bouaghi, Algeria

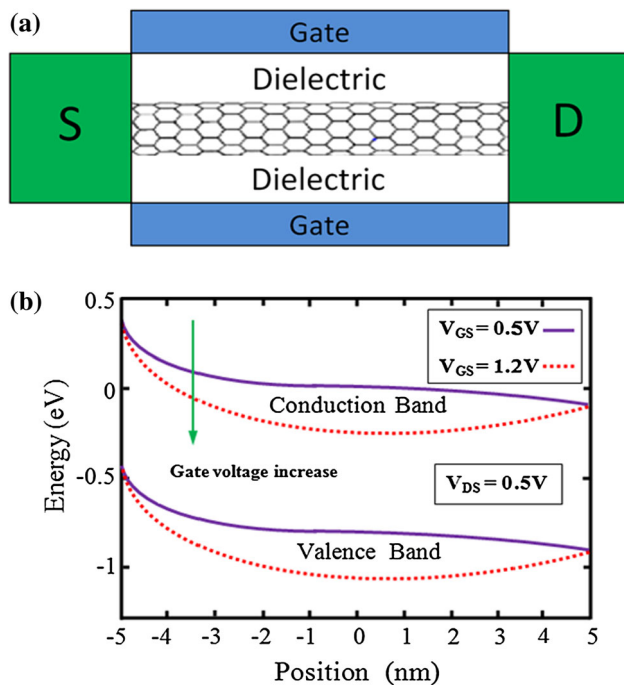


Fig. 1 Schottky barrier CNTFET, **a** 2-D cross section of the coaxial structure with intrinsic CNT as the channel and metal source/drain contacts, **b** energy band diagram obtained from Poisson equation. The metal Fermi level is taken to be at the midgap of the CNT [16]

One of the important aspects of nanotube transistors is the ambipolarity or unipolarity of their current–voltage characteristics. SB-CNTFETs exhibit strong ambipolar behavior; they show electron conduction at high gate voltages and hole conduction at low gate voltages. Recently, CNTFETs with zero or slightly negative Schottky barriers were achieved by attaching an intrinsic nanotube channel to the high work-function metal contacts [7]. When the gate oxide is thick, reducing the Schottky barrier height to zero suppresses the ambipolar conduction, but for the thin gate oxide, the transistor is still ambipolar, even if the Schottky barrier height for electrons/holes is zero [15]. Ambipolar conduction leads to a large leakage current that exponentially increases with the power supply voltage, especially when the tube diameter is large. Figure 1 shows a coaxial CNTFETs with a (13, 0) zigzag CNT as the channel which corresponds to a bandgap of about 0.83 eV and a diameter of 1 nm [16]. The gate is 10 nm long and wrapped around the channel. The gate thickness is assumed 6 nm. SB-CNTFET employs an intrinsic CNT and 20 nm long metallic contacts as the source and drain.

The energy bands for low and high gate voltages and the Schottky barriers are shown in Fig. 1b.

However, for MOSFET-like CNTFETs, only a positive gate voltage increases the current, because of the lowering of the barrier in the channel [16]. The energy bands for low and high gate voltages and the potential barrier in the channel are shown in Fig. 2.

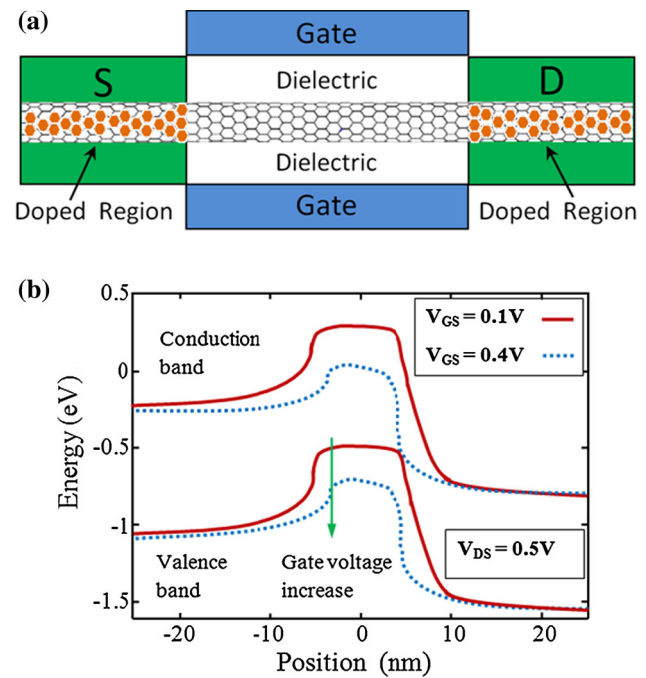


Fig. 2 MOSFET-like CNTFET, **a** 2-D cross section of the coaxial structure with intrinsic CNT as the channel and doped CNT sections as source/drain contacts, **b** energy band diagram obtained from Poisson equation [16]

It is clear from the figures why the characteristics of these two transistors differ. The current–voltage characteristics of the devices have been compared. Ambipolar behavior of the SB-CNTFETs constraints the use of these transistors in conventional CMOS logic families [17]. Methods have been proposed to reduce or eliminate the ambipolarity in CNTFETs. One of them uses asymmetrical contact types to introduce Schottky-ohmic CNTFET, which has a Schottky barrier at the CNT-metal interface at the source and an ohmic contact at the drain at the channel-doped CNT interface [18–20].

However, the device still suffers from band to band tunneling. That is, in low or negative voltages the electrons from the valence band can tunnel to the conduction band and contribute to the total current of the transistor and cause the increase of the current in negative voltages [21]. On the other hand, an advantage of ambipolar SB-CNTFETs is that they can be used as either an *n*-type or *p*-type FET in a CMOS application [22]. In MOSFET-like CNTFETs with heavily doped source and drain regions, when applying a negative gate voltage, the band to band tunneling may lead to ambipolarity. For suppressing this effect in MOSFET-like CNTFETs, it has been proposed [16] a non-uniform doping profile as shown in Fig. 3. This reduces the gradient of the channel potential barrier at each interface between the intrinsic and doped sections of the CNT and suppresses the band to band tunneling and ambipolar conduction.

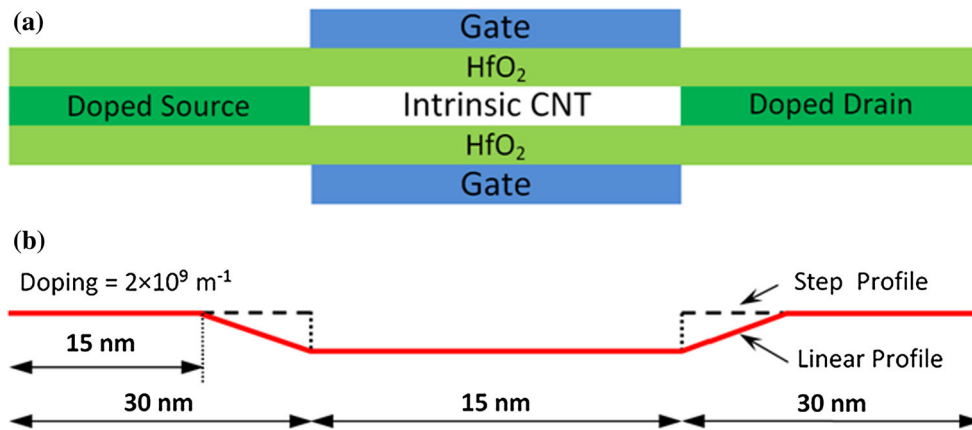


Fig. 3 a Cross section of the CNTFET. b Step and linear doping profiles for the MOSFET-like structure versus position

In this paper, we have studied the effect of physical and geometrical parameters on the performance of the SB-CNTFET. The relationship between the pass state current and the blocked state current is an essential factor for improved static performance of SB-CNTFET. The limitation of the use of this transistor is due generally to the effects of the height of the Schottky barrier, nanotube diameter and the capacity of the oxide layer. For this reason, we study the effect of the height of Schottky barrier on the pass state current. For dynamic system, we study the effect of the gate–source voltage, the chirality and the CNT diameter on the transition frequency.

2 Mathematical formulation

A carbon nanotube transistor is formed by two metal contacts, metal/nanotube in drain and source sides. The nature of the metal may be either aluminum (Al), titanium (Ti) [23], palladium (Pd) [14,24], or scandium (Sc). Platinum (Pt) is often used since it has poor wettability with the carbon nanotubes [14]. Because it has low adhesion energy, at the interfaces formed by the metal and the semiconductor nanotube contact, barriers of potential are formed and opposed to the carriers transition between source and drain through the nanotube channel. Thus, these barriers have an important role in determining the current since they determine the number of carriers present on the metal side and transmitted in the channel [25].

A polarization change of the gate or the drain affects the channel potential, and affects also the dimensions (height and width) of the two Schottky barriers. Generally, the profile of the band gap close to the contact depends strongly on the polarizations V_{GS} and V_{DS} . Figure 4 shows a SB-CNTFET structure in “back-gate” configuration for different polarization schemes V_{GS} and V_{DS} . In this example, only the first energy band is shown. Let’s examine the variation of

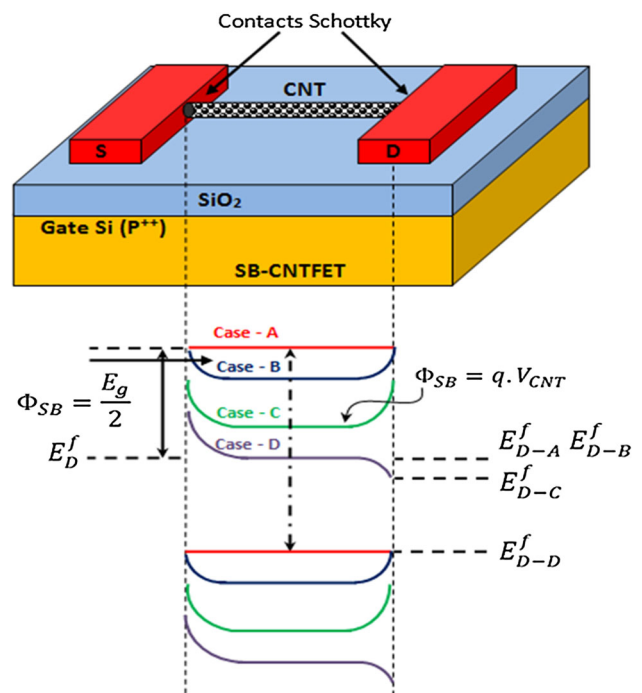


Fig. 4 Schematic representation of bands energy between source and drain of a SB-CNTFET in back gate (top) configuration for different regimes of polarization bands (Case A: $V_{DS} = V_{GS} = 0$, Case B: $V_{GS} > 0$ $V_{DS} = 0$, Case C: $V_{GS} > V_{DS} > 0$ and Case D: $V_{DS} > V_{GS} > 0$), only the 1st sub-band is shown [26]

the energy band profile and shape of the Schottky barriers depending on the range bias V_{GS} and V_{DS} .

3 Equivalent electrical circuit

The equivalent electrical circuit for the SB-CNTFET in Fig. 5 follows from the equations of the density of source and drain; Q_{QS} and Q_{QD} , (Eq. 1) and drain current (Eq. 2).

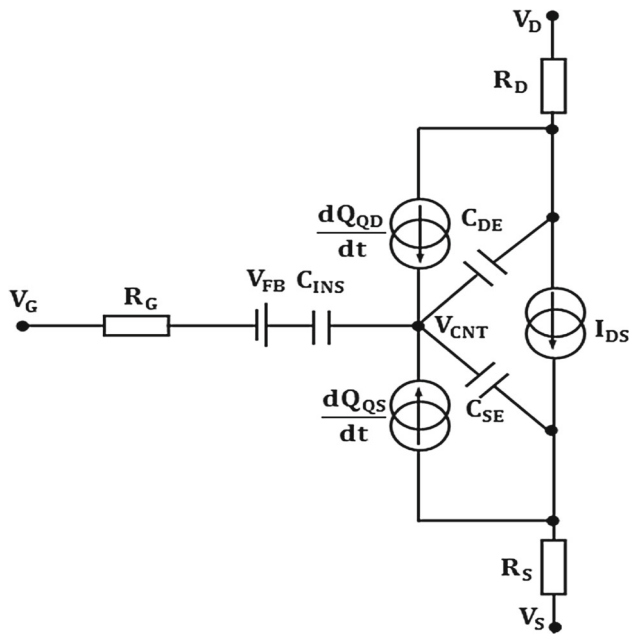


Fig. 5 Schematic of the equivalent model of the carbon nanotube transistor with modulated height barrier

$$Q_{S,D} = f_{SMO} Q_{low\ energy} + (1 - f_{SMO}) Q_{high\ energy} \quad (1)$$

$$I_D = \frac{4ek_B T}{h} \sum_{p=1}^{nb-sbbd} \left[\ln \left[1 + \exp \frac{eV_s + \Phi_{SB}^{eff} - sbbd[p]}{k_B T} \right] - \ln \left[1 + \exp \frac{eV_D + \Phi_{SB}^{eff} - sbbd[p]}{k_B T} \right] \right] \quad (2)$$

C_{INS} is the capacity of the gate oxide, it depends on the geometry and the dielectric constant of the insulator; V_{FB} is the voltage of flat bands, which takes into account the difference between the work function of the metal and the electron affinity of the nanotube; R_G is the access gate resistance; R_S and R_D are the access resistance of source and drain; C_{SE} and C_{DE} are the electrostatic capacity, which represent the change in the load interfaces doped nanotube/intrinsic nanotube [27]. The AC system, which is obtained from the equivalent circuit and the influence of the barrier Schottky is introduced into the calculation of the current I_{DS} and charge densities Q_{QS} and Q_{QD} [28].

3.1 Current calculation

Drain current in a SB-CNTFET is calculated by using the following equation:

$$I_{DS} = \frac{2e}{2\pi} M \left[\int_0^\infty v(k) f_s(k) T_s(E) dk - \int_{-\infty}^0 v(k) f_D(k) T_D(E) dk \right] \quad (3)$$

Ferry [29] assumes a one-dimensional (1D) channel, which is characterized by a ballistic transport between source and drain [30,31]. Thus, it is given by using the formulation of the effective Schottky barrier:

$$I_s = \frac{4e}{h} \sum_{p=1}^{nb-sbbd} \left[\int_{sbbd[p]}^\infty \frac{1}{1 + \exp \left(\frac{E - e(V_{CNT} - v_s)}{k_B T} \right)} \exp \left(-4 \frac{\sqrt{2m}}{3\hbar q E_{doc}} \right) (\Phi_{SB} - E - qV_s)^{\frac{3}{2}} dE \right] \quad (4)$$

$$I_{DS} = \frac{2e}{h} M \sum_{p=1}^{nb-sbbd} \left[\int_{\Phi_{SB}^{eff}}^\infty f_s(E) dE - \int_{\Phi_{SB}^{eff}}^\infty f_D(E) dE \right] \quad (5)$$

$$I_{DS} = \frac{4e}{h} \sum_{p=1}^{nb-sbbd} \left[\int_{\Phi_{SB}}^\infty \frac{1}{1 + \exp \left(\frac{E - e(V_{CNT} - v_S)}{k_B T} \right)} dE - \int_{\Phi_{SB}}^\infty \frac{1}{1 + \exp \left(\frac{E - e(V_{CNT} - v_D)}{k_B T} \right)} dE \right] \quad (6)$$

The $sbbd$ energy is the minimum of a sub-band with respect to the Fermi level of the carbon. We can integrate the current.

$$I_D = \frac{4ek_B T}{h} \sum_{p=1}^{-sbbd} \left[\ln \left[1 + \exp \frac{eV_s + \Phi_{SB}^{eff} - sbbd[p]}{k_B T} \right] - \ln \left[1 + \exp \frac{eV_D + \Phi_{SB}^{eff} - sbbd[p]}{k_B T} \right] \right] \quad (7)$$

with Φ_{SB-S}^{eff} and Φ_{SB-D}^{eff} barrier heights of the source and drain, respectively, and defined as

$$\Phi_{SB,S,D}^{eff} = (\Phi_{SB} - (sbbd[p] - eV_{CNT} + V_{S,D})) \exp \left(\frac{-d_{tunnel}}{\lambda_{Schottky}} \right) + (sbbd[p] - eV_{CNT} + V_{S,D}) \exp \left(\frac{-d_{tunnel}}{\lambda_{Schottky}} \right) + (sbbd[p] - eV_{CNT} + V_{S,D}) \quad (8)$$

In the case of field effect transistors, the transition frequency f_T is expressed as:

$$f_T = \frac{1}{2\pi} \frac{g_m}{c_g} \Big|_{V_{DS} - V_{DD}} \quad (9)$$

c_g is the intrinsic capacitance of the gate.

With the transconductance g_m representing the variation of the current in the channel as a function of gate voltage V_{GS} :

$$g_m = \frac{\partial I_D}{\partial V_{GS}} \tag{10}$$

4 Results and discussion

In this section, we will study the effect of physical and geometrical parameters on the performances of the SB-CNTFET. We consider only one sub-band, and we are limited to study the effect of the Schottky barrier and oxide layer as material parameters and the carbon nanotube diameter as the geometrical parameter. For a dynamic system we will study the effect of the gate–source voltage, the chirality, and the CNT diameter on the transition frequency.

Figure 6 shows the change in leakage current I_{DS} with the gate voltage V_{GS} , for three values of Schottky barrier height $\Phi_{SB} = 0.3, 0.5,$ and 0.6 eV (while keeping the other parameters constant). From this figure, it is clear that for negative values of the gate voltage ($V_{GS} \leq 0$), the current degrades almost linear and tends to zero, which is the dominant effect of ($V_{GS} \leq 0$) represented by a weakening of the intensity of the drain current. On the other hand, when the gate voltage increases ($V_{GS} > 0$), the drain current of a virtually linear course rises. We find that the conduction current I_{DS} is reduced as the barrier Φ_{SB} is increased, which leads to a low static conduction.

In Fig. 7, we plot the variations of the on state current I_{ON} versus the barrier height Φ_{SB} . We note that as the value of the barrier height increases, the on-state current decreases exponentially, which affects directly the static performance of the SB-CNTFET.

Figure 8 shows the drain current (I_{DS}) versus the gate voltage (V_{GS}) for SB-CNTFET with two different drain voltage (V_{DS}), i.e. 0.1 V and 0.6 V and two chirality values (13, 0) and (19, 0). Since this type of device works on tunneling from SB, there is great influence of V_{DS} on transfer characteris-

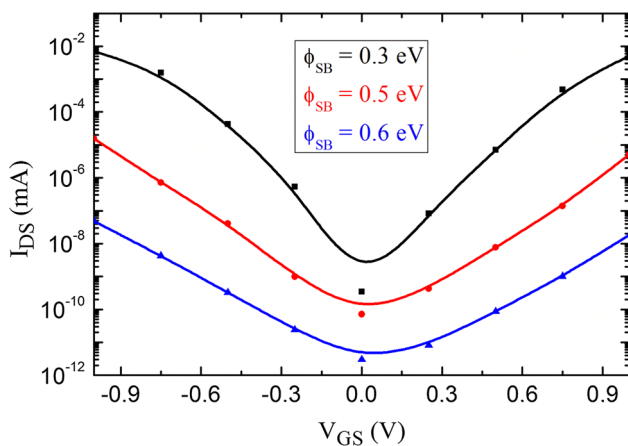


Fig. 6 The variation of the drain current I_{DS} versus gate voltage V_{GS} , for three values of Schottky barrier height $\Phi_{SB} = [0.3, 0.5, 0.6]$ eV

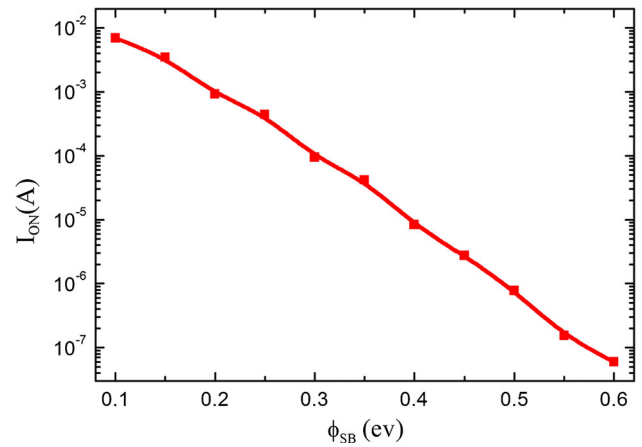


Fig. 7 The variation of the current in the on state I_{ON} versus the barrier height Φ_{SB}

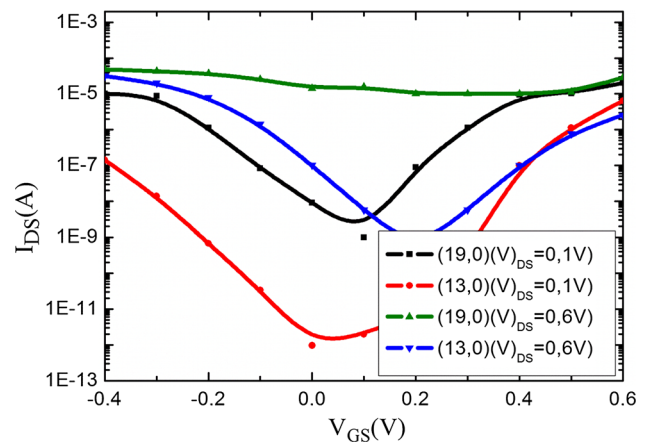


Fig. 8 The characteristics $I_{DS} - V_{GS}$ for two chirality values (13, 0) and (19, 0), and two values of V_{DS} (0.1 and 0.6 V)

tics. As CNT is throughout intrinsic, it behaves as both n -type and p -type for both positive and negative gate bias (ambipolar effect). When the device works under the subthreshold region, ($V_{DS} = 0.1$ V) it works n -type as we increase gate bias. But when it works under the saturation region there is great influence of V_{DS} . There is a very low I_{OFF} in this case, and the threshold voltage is much greater than the subthreshold region, which changes with increased V_{DS} . It is also clear that increasing the diameter of the channel will increase the conduction current, which is expected because the rate of passage of electrons is proportional to the diameter of the carbon nanotube.

Now in Fig. 9, we plot the variations of I_{ON}/I_{OFF} ratio with respect to the variation of oxide EOT thickness. I_{ON} and I_{OFF} are calculated for a given V_{GS} and V_{DS} . It can be seen from the figure that with decrement of EOT, the I_{ON}/I_{OFF} ratio increases and lead to a high on-state current. This is associated with superior control of the gate voltage over the channel, which helps in reducing the off-state current. As

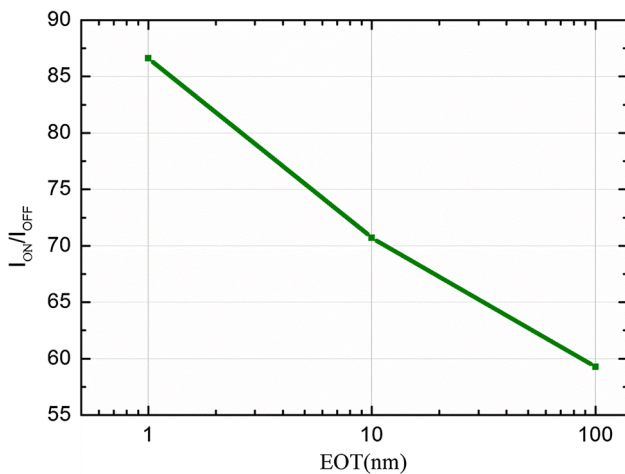


Fig. 9 The characteristics I_{ON}/I_{OFF} versus the EOT thickness

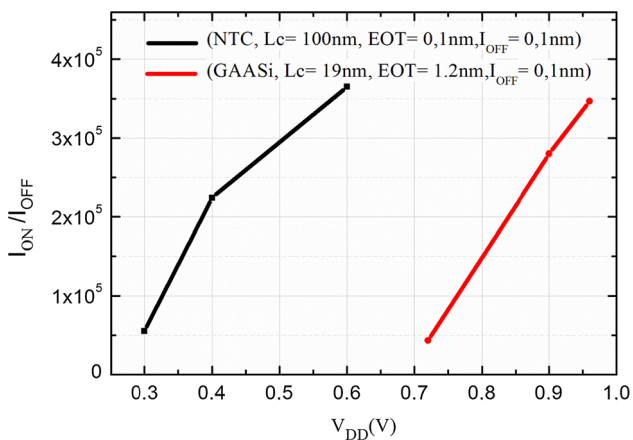


Fig. 10 I_{ON}/I_{OFF} ratio as a function of the power supply voltage for a SB-CNTFET with a CNT of thickness $EOT=0.1$ nm and channel length $L_g=100$ nm

the on-state current largely depends upon the higher energy level and flow of thermionic emission current, it becomes insensitive for device parameter compared to I_{OFF} [32]. We observe also an important linear variation of I_{ON}/I_{OFF} ratio in the range $1 \text{ nm} < EOT < 10 \text{ nm}$, this linear variation will be lower in the range $10 \text{ nm} < EOT < 100 \text{ nm}$, which leads to an improvement of the static performance when the EOT thickness is lowered [32].

Figure 10 shows the I_{ON}/I_{OFF} ratio as a function of the power supply voltage for a channel length $L_g=100$ nm and $EOT=0.1$ nm. From this figure we can observe that by increasing the power supply voltage, there is a linear evolution of the ratio I_{ON}/I_{OFF} , the slope decreases beyond 0.4 V, which explains the saturation current. When increasing power supply voltage, the off current, I_{OFF} increases. This phenomena is also reported experimentally by [15] and theoretically by atomistic scale simulations [19]. However, by increasing the power supply voltage, there is an increase on

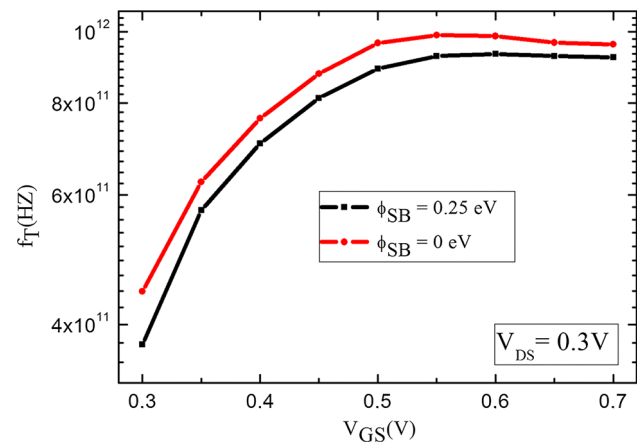


Fig. 11 Transition frequency f_T as a function of the gate voltage for two Schottky barrier heights Φ_{SB} of 0.275 and 0 eV and $V_{DS} = 0.3$ V

I_{ON} . High I_{OFF} values are important for switching speed. Also, for low power applications, designers should take care of V_{DD} voltage to keep large I_{ON}/I_{OFF} ratio. The off current increases faster with V_{DD} than the on-current [27].

In this section, we investigate the influence of physical and geometric parameters on the dynamic performance of the SB-CNTFET.

This study is limited to materials parameters (Schottky barrier Φ_{SB} , the oxide layer EOT), and geometric parameters (the carbon nanotube diameter).

Regarding Fig. 11, which plots the cut-off frequency as a function of gate voltage, we observe that decreasing the Schottky barrier height provides better dynamic performance. For the two barriers and for low values of V_{GS} , the two curves of transition frequency show nearly linear characteristics, which verify formula (9) with c_g ineffective. For medium values of V_{GS} , the c_g effect is dominant and the frequency f_T varies exponentially. For high values of V_{GS} , the transition frequency f_T is almost constant. Furthermore, when the SB height is reduced, the better saturation of drain current gives a weaker dependence of f_T on V_{DS} , and the behavior of f_T becomes similar to that of ohmic-contact CNTFE. However, thanks to smaller gate capacitance in Schottky devices, the maximum transition frequency f_{Tmax} is similar in ohmic and SB. In spite of drawbacks related to the ambipolar behavior (poor saturation of the $I_{DS} - V_{DS}$ characteristics and strong V_{DS} dependence of f_T), SB-CNTFET may provide performance similar to that of ohmic contact devices [33]. It makes thus possible to envision the design of new multi-function logic circuits taking advantage of ambipolar transport [34].

Figure 12 shows the variation of the maximum transition frequency f_{Tmax} as a function of four chirality: (10, 0), (13, 0), (16, 0), and (19, 0) at $V_{DS} = 0, 4$ V. From the figure, it is clear that the transition frequency f_{Tmax} is almost two times higher for a chirality of (19, 0) than the chirality of (10, 0).

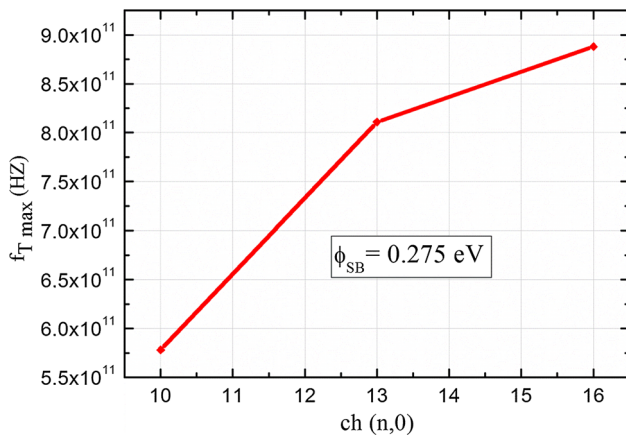


Fig. 12 Maximum transition frequency f_{Tmax} as a function of chirality of 4 nanotube (10, 0), (13, 0), (16, 0) et (19, 0) for $\Phi_{SB} = 0.275$ eV and $V_{DS} = 0.4$ V

Thus, the best transition frequencies are established for the large diameters of the nanotube. This variation of dynamic performances with the diameter of the nanotube contradicts with the static performances and the I_{ON}/I_{OFF} ratio which deteriorate for the largest diameters of the nanotube. This shows that it is necessary to establish a compromise for the choice of the diameter of the nanotube [27].

5 Conclusion

In this paper, a study of the influence of the parameters of a compact model of a SB-CNTFET transistor (height of the Schottky barrier, equivalent oxide thickness and nanotube diameter) was carried out in order to show their impact on the static and dynamic performances of the SB-CNTFET transistor. The analysis indicates that the SB-CNTFET static performances are affected by the height of the barrier Φ_{SB} . Other results show that the current I_{OFF} is increased with the increase of the diameter of SB-CNTFET. We also demonstrate that the I_{ON}/I_{OFF} ratio is increased with the decrease of the EOT thickness, which enhances the static performances of SB-CNTFET.

Further results showed that the transition frequency f_T degrades with the increase of the Schottky barrier height. This is related to the quality of the I_D versus V_{GS} that is to say to the transconductance which is increasingly degraded for the heights of Schottky barriers. This shows the great importance of the restriction of this material parameter to keep the static and dynamic performances of SB-CNTFET very high. We also show that the decrease of oxide thickness makes the I_{ON}/I_{OFF} ratio increases and lead to a high on-state current.

We also found that for CNTs with large diameters, the dynamic performances of the SB-CNTFET are enhanced

(increase of the transition frequency) but the static performances (decrease of I_{ON}/I_{OFF} ratio) are degraded. Consequently, the choice of the thin oxide and a compromise for the choice of the diameter of the nanotube may lead to high static and dynamic performances of SB-CNTFET.

References

- Dürkop, T., Kim, B.M., Fuhrer, M.S.: Properties and applications of high-mobility semiconducting nanotubes. *J. Phys. Condens. Matter* **16**(18), R553 (2004)
- Kim, B.M., Brintlinger, T., Cobas, E., Zheng, H., Fuhrer, M.S., Yu, Z., Droopad, R., Ramdani, J., Eisenbeiser, K.: High-performance carbon nanotube transistors on SrTiO₃/Si substrates. *Appl. Phys. Lett.* **84**(11), 1946 (2004)
- Javey, A., Guo, J., Paulsson, M., Wang, Q., Mann, D., Lundstrom, M., Dai, H.: High-field quasiballistic transport in short carbon nanotubes. *Phys. Rev. Lett.* **92**(10), 106804 (2004)
- Appenzeller, J., Lin, Y., Knoch, J., Avouris, P.: Band-to-band tunneling in carbon nanotube field-effect transistors. *Phys. Rev. Lett.* **93**(19), 196805 (2004)
- Morita, T., Singh, V., Oku, S., Nagamatsu, S., Takashima, W., Hayase, S., Kaneto, K.: Ambipolar transport in bilayer organic field-effect transistor based on poly(3-hexylthiophene) and fullerene derivatives. *Jpn. J. Appl. Phys.* **49**, 041601 (2010)
- Appenzeller, J., Knoch, J., Derycke, V., Martel, R., Wind, S., Avouris, P.: Field-modulated carrier transport in carbon nanotube transistors. *Phys. Rev. Lett.* **89**(12), 126801 (2002)
- Javey, A., Guo, J., Wang, Q., Lundstrom, M., Dai, H.: Ballistic carbon nanotube field-effect transistors. *Nature* **424**(6949), 654–657 (2003)
- Appenzeller, J., Knoch, J., Radosavljevic, M., Avouris, P.: Multimode transport in Schottky-barrier carbon-nanotube field-effect transistors. *Phys. Rev. Lett.* **92**(22), 226802 (2004)
- Radosavljevic, M., Heinze, S., Tersoff, J., Avouris, P.: Drain voltage scaling in carbon nanotube transistors. *Appl. Phys. Lett.* **83**(12), 2435 (2003)
- Javey, A., Guo, J., Farmer, D., Wang, Q., Yenilmez, E., Gordon, R., Lundstrom, M., Dai, H.: Self-aligned ballistic molecular transistors and electrically parallel nanotube arrays. *Nano Lett.* **4**(7), 1319–1322 (2004)
- Chen, J., Clinke, C., Afzali, A., Avouris, P.: Air-stable chemical doping of carbon nanotube transistors. In: *Proceeding on Device Research Conference*, pp. 137–138 (2004)
- Javey, A., Tu, R., Farmer, D.B., Guo, J., Gordon, R.G., Dai, H.: High performance *n*-type carbon nanotube field-effect transistors with chemically doped contacts. *Nano Lett.* **5**(2), 345–348 (2005)
- Raychowdhury, A., Keshavarzi, A., Kurtin, J., De, V., Roy, K.: Carbon nanotube field-effect transistors for high-performance digital circuits—DC analysis and modeling toward optimum transistor structure. *IEEE Trans. Electron Devices.* **53**(11), 2711–2717 (2006)
- Bhargava, K., Singh, V.: Electrical characterization and parameter extraction of organic thin film transistors using two dimensional numerical simulations. *J. Comput. Electron.* **13**, 585–592 (2014)
- Radosavljevic, M., Heinze, S., Tersoff, J., Avouris, P.: Drain voltage scaling in carbon nanotube transistors. *Appl. Phys. Lett.* **83**, 2435 (2003)
- Kordrostami, Z., Sheikhi, M.H.: *Fundamental Physical Aspects of Carbon Nanotube Transistors*. INTECH Open Access Publisher, Rijeka, Croatia (2010)
- Wang, W., Yang, X., Li, N., Xiao, G., Jiang, S., Xia, C., Wang, Y.: Transport study of gate and channel engineering on the

- surrounding-gate CNTFETs based on NEGF quantum theory. *J. Comput. Electron.* **13**, 192–197 (2014)
18. Kordrostami, Z., Hassaninia, I., Sheikhi, M.H.: Unipolar Schottky-Ohmic carbon nanotube field effect transistor. In: 3rd IEEE International Conference on Nano/Micro Engineered and Molecular Systems, NEMS 2008. IEEE (2008)
 19. Guo, J., Datta, S., Lundstrom, M.: A numerical study of scaling issues for Schottky-barrier carbon nanotube transistors. *IEEE Trans. Electron Dev.* **51**, 172–177 (2004)
 20. Subhagit, D., Debaprasad, D., Rahaman, H.: Design of 9-transistor content addressable memory cells using Schottky-barrier carbon nanotube field effect transistors. In: IEEE 2016 International Conference on Microelectronics, Computing and Communications (MicroCom), pp. 23–25. Durgapur, India (2016)
 21. Geetha, P., WahidaBanu, R.S.D.: A compact modelling of double-walled gate wrap around carbon nanotube array field effect transistors. *J. Comput. Electron.* **13**, 900–916 (2014)
 22. Guo, J., Lundstrom, M.: *Device Simulation of SWNT-FETs. Carbon Nanotube Electronics.* Springer, New York (2009)
 23. Appenzeller, J., Lin, Y.M., Knoch, J., Chen, Z., Avouris, P.: Comparing carbon nanotube transistors—the ideal choice: a novel tunneling device design. *IEEE Trans. Electron Dev.* **52**(12), 2568–2576 (2005)
 24. Colinge, J.P.: *Silicon-on-Insulator Technology: Materials to VLSI.* Kluwer Academic, Norwell, MA (1991)
 25. Knoch, J., Zhang, M., Mantl, S., Appenzeller, J.: On the performance of single-gated ultrathin-body SOI Schottky-barrier MOSFETs. *IEEE Trans. Electron Dev.* **53**(7), 1669–1674 (2006)
 26. Diabi, A., Hocini, A.: Compact modeling of the performance of SB-CNTFET as a function of geometrical and physical parameters. *Acta Phys. Pol. A* **127**(4), 1124–1127 (2015)
 27. Najari, M., Frégonèse, S., Maneux, C., Mnif, H., Masmoudi, N., Zimmer, T.: Schottky barrier carbon nanotube transistor: compact modeling, scaling study, and circuit design applications. *IEEE Trans. Electron Dev.* **58**(1), 195–205 (2011)
 28. Hasan, S., Salahuddin, S., Vaidyanathan, M., Alam, M.A.: High-frequency performance projections for ballistic carbon-nanotube transistors. *IEEE Trans. Nanotechnol. Nanotechnol.* **5**(1), 14–22 (2006)
 29. Ferry, D., Stephen, K., Goodnick, M., Bird, J.: *Transport in Nanostructures.* Cambridge University Press, Cambridge (2009)
 30. Datta, S.: *Electronic Transport in Mesoscopic Systems.* Cambridge University Press, Cambridge (1997)
 31. Sze, S.: *Physics of Semiconductor Devices.* Wiley, Hoboken (2007)
 32. Shirazi, S.G., Mirzakuchki, S.: Dependence of carbon nanotube field effect transistors performance on doping level of channel at different diameters: on/off current ratio. *Appl. Phys. Lett.* **99**(26), 263104–263104 (2011)
 33. Maneux, C., Fregonese, S., Zimmer, T., Retailleau, S., Nguyen, H.N., Querlioz, D., Bournel, A., Dollfus, P., Triozon, F., Niquet, Y.M., Roche, S.: Schottky barrier carbon nanotube transistor: compact modeling, scaling study, and circuit design applications. *Solid-State Electron.* **89**, 26–67 (2013)
 34. Yu, W.J., Kim, U.J., Kang, B.R., Lee, I.H., Lee, E., Lee, Y.H.: Adaptive logic circuits with doping-free ambipolar carbon nanotube transistors. *Nano Lett.* **9**, 1401–1405 (2009)